PHYSICAL REVIEW B VOLUME 34, NUMBER 11 1 DECEMBER 1986

Numerical study of the growth kinetics for a Langevin equation

Oriol T. Valls
School of Physics and Astronomy, University of Minnesota, Minneapolis, Minnesota 55455

Gene F. Mazenko
The James Franck Institute and Department of Physics, The University of Chicago, Chicago, Illinois 60637
(Received 28 April 1986)

We study the growth kinetics of a time-dependent Ginzburg-Landau model appropriate for the dynamics of a simple order-disorder transition by direct numerical solution of the associated Langevin equation. Our results are consistent with the Lifshitz-Cahn-Allen theory of curvature-driven dynamics. Our calculations indicate that such methods can be used to analyze more sophisticated models, and that they are at least competitive with Monte Carlo simulations.

I. INTRODUCTION

We study here the growth kinetics of an order-disorder transition by direct numerical solution of the appropriate Langevin equation. This work is, to some degree, of a preliminary nature since one of our purposes is to investigate the power and capabilities of the direct solution method, as compared, e.g., to Monte Carlo (MC) simulations. However, even at this level, we find a strong correspondence between the growth kinetics of this case and those generated by the extensively studied kinetic Ising models. Our calculations therefore serve as a test of the feasibility of using these methods to analyze more sophisticated models.

Only recently has it been appreciated that the growth kinetics of systems subjected to strong perturbations can be grouped into a relatively small number of classes. The parameters differentiating these classes are beginning to emerge. In particular, Ising-like systems quenched from a high temperature to some temperature below a transition temperature T_C show quite similar[1] behavior independent of the detailed nature of the dynamics used to generate the time evolution of the system. The difference in growth kinetics—how the system grows an ordered state from a disordered state—appears to depend only on rather general features of the system. It is well known that it is very important to distinguish the case where the order parameter is conserved from those cases where it is not. Among the variables which play a role in determining the growth kinetics classes are the number of phases that can coexist at low temperature,[2,3] the number of components of the order parameter,[4] and possibly whether the domain walls are hard or soft.[5] The constraint of a conservation law slows down the equilibration process considerably. By now much is understood about systems whose dynamics can be described by kinetic Ising models and a picture is emerging which explains the robust feature of the various growth kinetics classes. In Refs. 6 and 7 we have developed a theory in which the asymptotic behavior of the growth kinetics is understood in terms of attractive zero-temperature fixed points in a renormalization-group picture.

While the growth kinetics of systems with a discrete number of states (Ising, Potts, clock models) have been well investigated, rather little has been done about systems with more complicated order parameters and kinetics. The main reason for this is the appealing simplicity of the kinetic Ising models. Because of the finite-state nature of Ising and Potts models, these systems can be very conveniently simulated using Monte Carlo techniques. Such methods have been extremely useful since there is no obvious expansion parameter that can be used to develop analytical work. Much less attention has been paid to systems where the order parameter is more naturally treated as a continuous variable (a field) rather than a discrete variable. One expects the symmetry of the order parameter (spin waves in the case of a broken continuous symmetry) and "mode" coupling nonlinearities to play an important role in the analysis. One knows, for example, that flow is an important element in treating the hydrodynamics of fluids. Although we shall not focus on it in this paper, one of the intriguing questions which can be addressed using these techniques will be the existence and annealing of trapped defects after quenching. For example, how much vorticity is trapped in helium after it has been rapidly quenched below the lambda transition. Very little quantitative work has been carried out on these questions.

While it has seemed natural to use simulation methods for treating systems with continuous order parameters of the type mentioned in the paragraphs above, previous efforts have not been particularly encouraging. The difficulty is that the amount of computing needed to obtain comparable results is much larger, for example, for the scalar order parameter Langevin equation than for a single-spin-flip kinetic Ising model (SFKI). It has only recently been appreciated how much computing is really necessary in order to obtain quantitative results for local quantities, even for the SFKI model. Often one needs hundreds of runs for a given quantity before one has sam-

pled enough initial conditions to give quantitative results. For the Langevin equation, since it contains a random Gaussian field, one must solve it many times and average the solutions. Each solution (or trajectory) may be thought of as a "run," and one again needs a fairly large number of runs. The main problem, however, is the need to carry out, in each trajectory, a fairly large amount of floating point arithmetic, including in particular the generation of the Gaussian noise fields. As we shall see below, these fields can be generated quite efficiently using the vectorizing capabilities of the Cray computers. Although some results for the conserved case have been obtained,[8] it appears that one has had to wait for the availability of large enough computers before such calculations could be made quantitative.

We treat here the simplest problem involving a quenched field: a Langevin equation driven by a Landau-Ginzburg free energy—model A in the nomenclature of Hohenberg and Halperin.[9] This is a model for a scalar, nonconserved order parameter. Much of the discussion (see Refs. 10–13) of this model has been of a phenomenological nature. There is a systematic calculation[4] for the N-vector model in the large-N limit, in which one recovers scaling behavior and the Lifshitz-Cahn-Allen (LCA) growth law for the time evolution of the average domain size $L(t)\simeq t^{1/2}$. This would seem to indicate that the LCA growth law holds for model A ($N=1$), but many other questions are pending. One of particular interest to us, but which will not be addressed here, is the following: How do those field theories fit into the renormalization-group picture of Ref. 7?

The simple model we treat here serves as a good first test case since we think that we know how it should behave. We expect that it belongs to the same class as the SFKI model. Indeed our results are consistent with the LCA growth law.

This paper is organized as follows. In the next section we specify the model and parameters chosen and the numerical techniques employed. The early time behavior is investigated analytically. Then, in Sec. III we present numerical results for several quantities of interest. We give a brief discussion of the phase diagram since the system studied here is more complicated than an Ising model. In particular, the equation of state and the transition temperature are now functions of the parameter θ which connects the Ising and "displacive" limits. We then show results for the time-dependent susceptibility $\chi(t)$ and the quasistatic structure factor $C(q,t)$. The latter quantity shows the expected development of a Bragg peak, as for the Ising model. From analyzing the peak in $C(q,t)$ we verify the LCA law. The spatial correlation function $C(r,t)$ is also studied. We point out that the zero-temperature limit must be handled with care.

As a result of our study we have gained some feeling for the statistics associated with the problem and the capabilities of new large-scale computing facilities. We note that direct brute force simulations, of the type carried out here, have not usually been conclusive. They must be used together with some theoretical development. Scaling analysis and renormalization-group methods have proved very useful in the Ising limit and we expect similar methods to work well also in the continuum case.

II. LANGEVIN EQUATIONS

A. Model

We consider a set of scalar fields $\psi_i(t)$ set on an $N\times N$ square lattice, in the range $-\infty<\psi_i<\infty$. We assume that in equilibrium the statistics of these fields is governed by an effective Hamiltonian or free energy $F[\psi]$ of the Ginzburg-Landau type:[14]

$$F[\psi]=\tfrac{1}{2}\sum_i\left[-r\psi_i^2+K'(\nabla\psi_i)^2+\frac{u}{4}\psi_i^4\right], \tag{2.1a}$$

where the i denote lattice sites and $(\nabla\psi_i)^2$ the discrete version of the squared gradient. Since the overall scale of $|\psi|^2$ is arbitrary, only two of the three parameters r, K', and u are independent. There does not seem to be a consensus in the literature as to how to choose these parameters. Petschek and Metiu (Ref. 8) chose the mean-field correlation length plus the Ginzburg criterion parameter. We choose here the parametrization used in Ref. 15 to obtain an approximate phase diagram, which is given by

$$F[\psi]=\frac{K}{2}\sum_i[-\theta\psi_i^2+(\nabla\psi_i)^2+\tfrac{1}{2}(1+\theta)\psi_i^4]\,. \tag{2.1b}$$

The general form (2.1a) can be put into the form (2.1b) by rescaling $|\psi|^2$ by a factor of $u/[2(|r|+K')]$. Then one has $\theta=|r|/K'$ and $K=2K'^2(1+\theta)/u$. The parameter θ can vary from 0 to ∞. In the limit $\theta\to\infty$, (2.1b) reduces to the Ising Hamiltonian, where K is the usual Ising coupling constant. In the $\theta\to 0$ limit one obtains a purely displacive free energy and no phase transition. Thus, the parameter θ measures the "Ising-like" or "displacivelike" quality of the system. Our numerical calculations have been performed using (2.1b).

By further rescaling $|\psi|^2$ by a factor of $\theta/(1+\theta)$, Eq. (2.1b) can be rewritten as

$$F[\tilde{\psi}]=\frac{\tilde{K}}{2}\sum_i[(\nabla\tilde{\psi}_i)^2+\tfrac{1}{2}\theta(\tilde{\psi}^2-1)^2], \tag{2.1c}$$

where $\tilde{K}=K\theta/(1+\theta)$. Note that a constant term has been added to obtain (2.1c), but this affects neither the statics nor the dynamics. The fact that $\theta\to\infty$ corresponds to the Ising limit is particularly transparent from (2.1b), but the displacive limit is quite different. A factor of the inverse temperature is customarily included in K. This factor will have to be considered explicitly later on, when it will be important to look at the low-temperature properties of the system. Thus, in (2.1b) and (2.1c), K is in units of the temperature.

The equilibrium properties of this system are given by averages of the form:

$$\langle A[\psi]\rangle=\int d\psi_1 d\psi_2\cdots A[\psi]e^{-F[\psi]}/Z\,, \tag{2.2}$$

where Z is the partition function obtained by choosing $A[\psi]=1$ and demanding $\langle 1\rangle=1$ in the equation above. The dynamics of this model are assumed to be generated by a Langevin equation of the form:

$$\frac{d\psi_i}{dt} = -\Gamma \frac{\delta F[\psi]}{\delta \psi_i} + \eta_i(t) , \tag{2.3}$$

where Γ is a kinetic coefficient and η_i is a Gaussian noise satisfying

$$\langle \eta_i(t)\eta_j(t') \rangle = 2\Gamma\delta_{ij}\delta(t-t') . \tag{2.4}$$

Inserting (2.1b) in (2.3), we have

$$\frac{d\psi_i}{dt} = \Gamma K[\theta\psi_i - (1+\theta)\psi_i^3 + \nabla^2\psi_i] + \eta_i , \tag{2.5}$$

where $\nabla^2\psi_i$ is the usual discrete version of the Laplacian:

$$\nabla^2\psi_i = \sum_a (\psi_{i+a} - \psi_i) \tag{2.6}$$

and a is a nearest-neighbor lattice vector. This completes the specification of our model. Note that the lattice constant is the unit of length. The physical quantities of interest in the context of a temperature quench are the correlation functions:

$$C_{ij}(t) = \langle \psi_i(t)\psi_j(t) \rangle , \tag{2.7}$$

where the average is over the noise and the initial probability distribution governing $\psi_i(0)$. The time t is measured from the time of the quench.

B. Methods

The first step in solving (2.5) numerically is to discretize the time into intervals δt. The presence of the random force severely restricts the numerical methods one can use in this case. The simplest procedure[8] is to use the Euler method, i.e.,

$$\psi_i(t+\delta t) = \psi_i(t) + \Gamma K \delta t[\theta\psi_i(t) - (1+\theta)\psi_i^3(t) + \nabla^2\psi_i] + \sqrt{2\delta t}\,\xi_i(t) , \tag{2.8}$$

where $\nabla^2\psi_i$ is given by (2.6) with four nearest neighbors and ξ_i is the discrete time version of the noise term, defined by $\xi_i(t) = \sqrt{(\delta t/2)}\eta_i(t)$, and satisfying

$$\langle \xi_i(t)\xi_j(t') \rangle = \Gamma\delta_{t,t'}\delta_{ij} . \tag{2.9}$$

To improve on this development, one can use a modified Euler or predictor corrector method. Instead of replacing the time derivative in the interval $(t, t+\delta t)$ by its value at t [as done in (2.8)], one replaces it by the average of its value at t and the value at $t+\delta t$ predicted by (2.8). In the presence of the random force there is no guarantee, as in its absence, that this procedure allows one to increase the interval δt, and indeed this does not appear to be the case. However, the resulting noise term involves a combination of $\xi_i(t)$ and $\xi_i(t+\delta t)$ and its root-mean-square average is smaller than Γ by a factor of $\sqrt{2}$. This allows for a reduction in the number of times the equation must be solved before convergence for the averaged results is obtained. However, this advantage is roughly cancelled by the necessity to perform more involved floating point arithmetic. For this reason we have used the simple Euler method, given by (2.8) in nearly all of our calculations. The modified method may turn out to be advantageous for other forms of the free energy.

The next question is the generation of the Gaussian random field $\xi_i(t)$ from the uniformly distributed random numbers generated by the computer. Many ways to accomplish this are available. A popular one is to write

$$\xi = \left[\frac{12}{M}\right]^{1/2} \sum_{j=1}^{M} (x_j - \tfrac{1}{2}) , \tag{2.10}$$

which, by the central limit theorem, generates a Gaussian distribution for ξ from a uniform distribution for the x_i for large M. $M=12$ is a common choice for obvious reasons. We have found, however, that we could obtain faster results by generating a single x_i and then numerically inverting the probability function.[16] The reason lies in the vector capabilities of the Cray computer: the whole field $\xi_i(t)$ can be generated by a single vectorizable loop, while generating twelve x_j in the same loop is apparently slower than doing the small amount of algebra required to invert the probability distribution. Thus, we have chosen the latter method, which also yields higher quality results, as determined by computing higher-order moments of the distribution.

Because of the random force and the random nature of the initial conditions, one obtains a different solution $\{\psi_i(t)\}$ of the system (2.5) for each set of initial conditions. Each solution is a trajectory in phase space. Clearly, one must collect the relevant information (in our case the correlation functions discussed in Sec. III) from every trajectory and then average over a sufficient number of trajectories. Informally, we will call the generation of each trajectory a "run."

We turn now to the initial conditions. In problems of interest one quenches from some initial, presumably equilibrium state, characterized by an initial temperature $T_I \propto 1/K_I$, to a final state characterized by a lower temperature $T_F \propto 1/K_F$. Unlike the Ising case, the high-temperature ($K_I \to 0$) limit of our model is not completely trivial, because of the θ variable. One cannot simply set $K_I = 0$ in the free energy since correlation functions such as

$$C_{ij} = \langle \psi_i\psi_j \rangle \tag{2.11}$$

will not be defined because the resulting integrals do not converge. If one makes the substitution:

$$\Phi_i = \tilde{\psi}_i \tilde{K}_I^{1/4} = \psi_i K_I \left[\frac{\theta_I}{1+\theta_I}\right]^{3/4} , \tag{2.12}$$

then the free energy can be put into the form

$$F[\Phi] = \tfrac{1}{2}\sum_i [\tilde{K}^{1/2}(\nabla\Phi_i)^2 + \tfrac{1}{2}\theta(\Phi_i^2 - \tilde{K}^{1/2})^2] \tag{2.13}$$

and

$$C_{ij} = \frac{1+\theta_I}{\theta_I} \langle \Phi_i\Phi_j \rangle / \tilde{K}_I^{1/2} . \tag{2.14}$$

For the system governing the Φ fields one can take the limit $\tilde{K}_I \to 0$ and obtain

$$C_{ij} = 2\delta_{ij}[(1+\theta_I)/\theta_I]\Gamma(3/4)/[(\tilde{K}_I\theta_I)^{1/2}\Gamma(1/4)] , \tag{2.15}$$

where the Γ's are the ordinary Γ functions. Thus C_{ij} increases with the square root of temperature for large temperatures. The initial state then corresponds to a set of uncorrelated spins which are distributed with a weight proportional to $\exp(-K_I\theta_I\psi_i^4)$.

It is obviously impractical (except in the Ising limit) to choose true infinite-temperature initial conditions (as usually done in Monte Carlo simulations of the Ising model) because a set of initial ψ_i uniformly distributed from $-\infty$ to $+\infty$ would pose considerable numerical difficulties. With no detriment to the physics, we have used three different kinds of initial conditions.

(i) Set all $\{\psi_i\}=0$ (as in Ref. 8). This condition does not correspond to any equilibrium point in phase space. Its appeal is its simplicity.

(ii) Random Ising initial conditions, $\{\psi_i^2=1\}$.

(iii) $\{\psi_i\}$ randomly and uniformly distributed in the range $[-\psi_0,\psi_0]$.

Choice (iii) would be the real $T_I\to\infty$ limit if $\psi_0\to\infty$, and it is a reasonable approximation to the equilibrium high-temperature case if we take $\psi_0^2=3C_{ii}$ where C_{ii} is given by (2.15). We have typically taken $\psi_0^2=3$. Choice (ii) corresponds to $C_{ij}=\delta_{ij}$ and choice (i) to $C_{ij}=0$. Note, however, that only for case (ii) is the initial system in thermal equilibrium at a definite point in the (K,θ) phase diagram.

We have found, however, that the behavior of the correlation functions is not affected by the choice of initial conditions except at very early times ($\Gamma t\ll 1$). Of course, the long-time growth law is, *a fortiori*, independent of the initial conditions as we shall see in Sec. III. This is as expected.

It is very useful to check our numerical technique against some exact results. If $u=0$ in (2.1a) then one easily obtains for $C(q,t)$ (the Fourier transform of C_{ij}):

$$C(q,t)=\frac{-1}{(-r+Kq_{\rm eff}^2)}(e^{-2\Gamma(-r+Kq_{\rm eff}^2)t}-1)\ , \tag{2.16}$$

where we have taken type (i) initial conditions and

$$q_{\rm eff}^2=4-2(\cos q_x+\cos q_y)\ . \tag{2.17}$$

For $r>0$, Eq. (2.16) represents an unstable system, growing exponentially for small enough q. We can, in principle, also check the early-time evolution which can be determined analytically. One can easily show (most conveniently using the Fokker-Planck representation for this problem), that

$$\frac{dC_{ij}(t)}{dt}=-2\Gamma\delta_{ij}-\Gamma\left\langle\psi_j\frac{\delta F}{\delta\psi_i}\right\rangle-\Gamma\left\langle\psi_i\frac{\delta F}{\delta\psi_j}\right\rangle\ , \tag{2.18}$$

where the averages are over the nonequilibrium probability distribution. If, however, we evaluate this expression at $t=0$, then the averages are over the initial equilibrium probability distribution characterized by K_I. Note that the $F\{\psi\}$, in the equation of motion above corresponds to K_F. Writing $F=(K_F/K_I)F_I$, one can easily derive the rather elegant results for quenches at constant θ from *equilibrium* conditions K_I to K_F:

$$\left.\frac{dC_{ij}(t)}{dt}\right|_{t=0}=-2\Gamma\delta_{ij}(K_I-K_F)/K_I\ . \tag{2.19}$$

For the initial conditions of types (i) and (ii) the initial derivative can be obtained directly from (2.18), which holds for arbitrary initial states.

Note that if the system is quenched with Ising initial conditions while keeping $\theta\to\infty$, it will not evolve in time since each variable is trapped at the bottom of an infinitely deep potential well.

III. RESULTS

The physical quantities of interest are the correlation functions $C_{ij}(t)$ or equivalently their Fourier transform $C(q,t)$ where q is an appropriate discrete wave vector in the first Brillouin zone. The lattice size employed in the bulk of the results reported here is 32×32. This choice represents a reasonable compromise between the amount of computing time needed for a run, and the need to have as large a system as possible. From the point of view of computing efficiency, one would like to collect all the products $\psi_i\psi_j$. This collection process can easily be vectorized and is, therefore, very fast. However, there are more than 10^6 such products (for $N=32$) and since the Cray 1 has memory "only" for about 4×10^6 floating points numbers, this collection could be done only for a very small number of runs (or, alternatively, of time bins). We can reduce the memory requirements (at the expense of slowing down the process) by taking advantage of the translational invariance of the system and grouping together all of the $\psi_i\psi_j$ with the same separation r_i-r_j. One has no such storage problems for the time-dependent susceptibility:

$$C(q=0)\equiv\chi(t)=\frac{1}{N^2}\sum_{i,j}C_{ij}(t)\ , \tag{3.1}$$

which can be collected very efficiently. For this reason we have more information on $\chi(t)$ than on the general $C(q,t)$.

We find, as expected, that the order in the system after the quench increases. The growth of order is best monitored by observing the peak in $C(q,t)$ that grows and narrows with time. After a time which depends on the quenching parameters but is typically of order $t\sim 4$ (we use units of time such as $\Gamma=1$ unless otherwise indicated), the typical domain size is comparable to 32, or, in other words the width $q_w(t)$ of the peak in $C(q,t)$ becomes of the order of the smallest nonzero wave vector in the Brillouin zone. We point out here that the relation between Langevin equation times and Monte Carlo steps in a corresponding Monte Carlo simulation is not trivial.[17] We will get into this question in more detail later, but as a simple guide, one Langevin time unit may be thought of as being on the order of 5000 MC steps per site. However, even after the domains have reached this size, $\chi(t)$ continues to grow until very few "domains" remain and finite-size saturation effects set in. The integration step δt required to obtain convergence is of order 0.01 when θ is of order unity, but it becomes very small if θ is too large.

The results reported here are average over a number of runs ranging from 30 to 90. The computer code needed to solve (2.8) by the methods indicated in Sec. II is not very complicated. As a check, we have verified that the $u=0$ limit (2.16) is properly reproduced at small q for type-(i) initial conditions. Equation (2.19) also gives a check when the u term is present, but only at times $t \ll 1/\theta$.

A preliminary step before quenching the system into the ordered region is to determine the line of critical points in the (K,θ) plane. We do this in the following fashion. For a given set of disordered initial conditions and a system of size N, we drive the system with the fixed final set of parameters K_F and θ_F and monitor the growth of $\chi(t)$. χ will typically grow rapidly with time showing a power-law behavior (the exponent will be analyzed below). Eventually, for large enough times χ saturates. We then increase the size of the system to $N' > N$ and repeat the analysis. If χ saturates at a value which is independent of N for large N, then the system equilibrates without ordering. If, however, one finds that the saturated value of χ is proportional of N^2, then one can conclude that the system has ordered for that choice of K_F and θ_F. Looking at Fig. 1, one can gain some idea about the ordering process by looking at longer times and by varying the size of the system treated. Fixing $K=1.75$ and $\theta=2.5$ and carrying out 30 runs for lattice sizes $N=8$, 16, 20, 32, one obtains the results shown. We easily see that there is a saturation effect for the smaller systems as expected. If one is in the ordered region then the growth continues until χ is of the order of the magnetization squared times N^2. We have performed this process by fixing θ and then varying K until we can clearly see that we have crossed the phase boundary. The values of θ chosen were 0.5, 1.5, 2.5, 4, 6.4, 12, and 20. (The larger values were used to verify that the Ising limit was correctly obtained.) There are

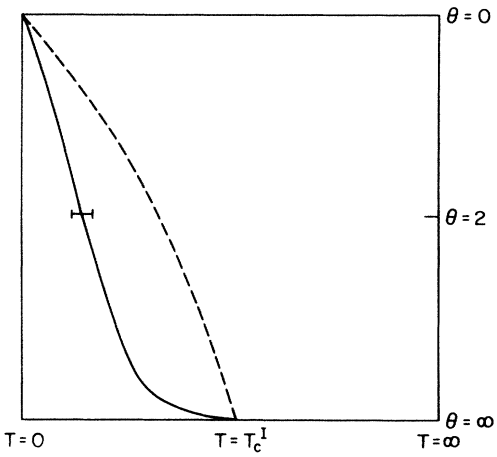

FIG. 2. The phase diagram in the (K,θ) plane. The x axis is $\tanh(1/4K)$ and the y axis is $1-\tanh(\theta/4)$, as in Ref. 15. The dashed line represents the results of Ref. 15 and the solid line the results of our present work.

enough values of θ to map out the approximate phase diagram (Fig. 2). Note that this diagram differs from the approximate renormalization-group (RG) result of Ref. 15. The error bars are due to the fact that near the transition it becomes impossible to verify, in a finite time, whether χ saturates. This is illustrated in Fig. 3 where results for 30 runs are shown for $\theta=12$ (very near the Ising line in Fig. 2, although the system is not really Ising-like, since amplitude fluctuations are still far from negligible). At $K_F=0.8$ the system is clearly ordered, while at $K_F=0.7$ one is extemely close to the transition. Note that our main purpose in determining the phase diagram was chiefly to make sure that we really quench into the ordered region, and that for this purpose a lower bound to the transition temperature suffices.

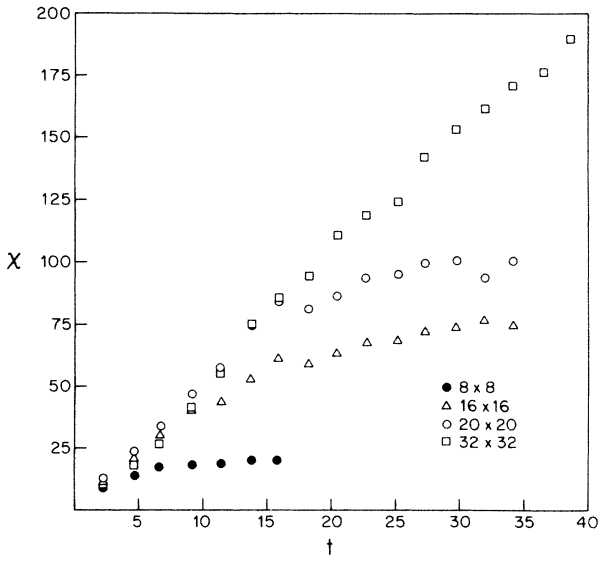

FIG. 1. Results for χ [defined in (3.1)] for quenches to $K=1.75$, $\theta=2.5$, and systems of different sizes as indicated. Each set of points represents an average over 30 trajectories. Note the linear growth followed by size-dependent saturation.

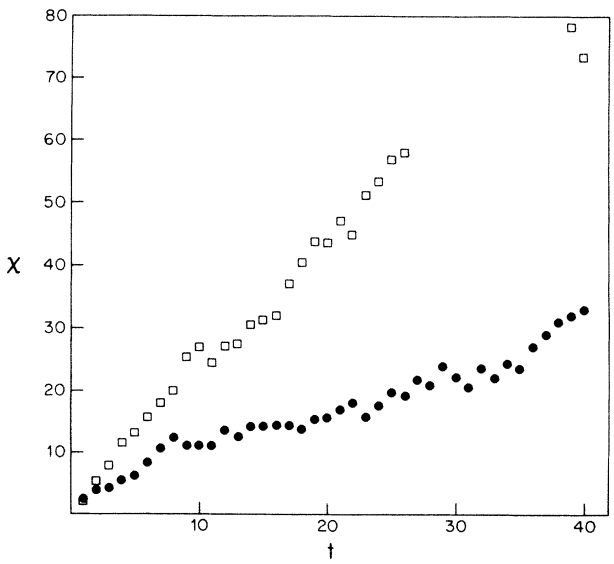

FIG. 3. Results (30 run averages) at $\theta=12$. For $K=0.8$ (squares), χ shows clear linear growth, while at $K=0.7$ (solid circles), which is very close to the transition line, the growth is very weak.

It is already evident from Fig. 1 that $\chi(t)$ grows linearly with time until saturation effects set in. A more careful examination of the data shows that for times $t > 0.2$, $\chi(t)$ can be fitted to a form:

$$\chi(t) = a(t - t_0) \ . \tag{3.2}$$

In Fig. 4 we show a typical example of $\chi(t)$ at intermediate times [while $q_w(t)$ is still narrowing]. Figure 4 represents 90 runs at $K = 1.75$, $\theta = 2.5$. A best fit of the data gives $a = 4.193$, $t_0 = 0.077$ (with coefficient of determination $r^2 = 0.997$). The scatter of the points in Fig. 4 is a measure of our statistical error. The small time t_0 is very sensitive to statistical error and we have not been able to determine whether it is a systematic function of K or θ.

The results of Figs. 3 and 4 correspond to $\{\psi\} = 0$ [type (i)] initial conditions. That this time regime is not appreciably affected by the boundary conditions is shown in Fig. 5 where results for 30 runs at each of the three kinds of initial conditions are shown. Clearly the memory of the initial conditions is lost, within statistical error, at the times of interest. This removes any worry associated with using initial conditions which do not correspond to a definite point in the phase diagram.

In order to gain a qualitative feeling for the ordering process, we show in Figs. 6 and 7 "pictures" of the ordering as a function of time. In Fig. 6, for $K = 1.75$ and $\theta = 2.5$, the evolution of a typical row of fields during a simulation are shown for a sequence of increasing times. One can see the evolving order—this particular row becoming part of a $\psi > 0$ domain. The conditions in Fig. 7 are the same as in Fig. 6 except that the whole lattice is plotted with a dot for a positive value of the field and a blank for a negative value of the field. Again, one clearly sees the ordering develop on comparing the two times.

The most direct method for the determination of the growth law comes from a direct analysis of $\chi(t)$ where

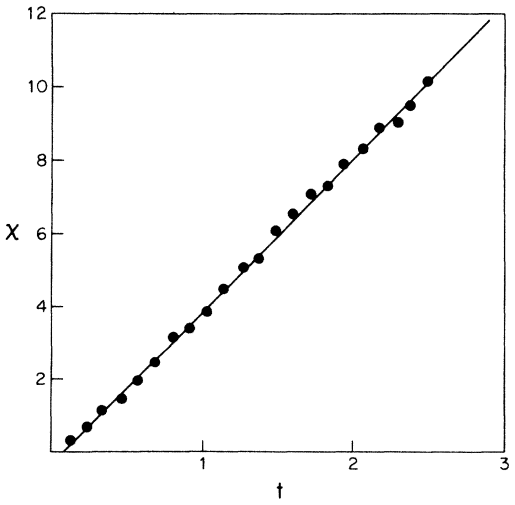

FIG. 4. Linear fit to $\chi(t)$ for quenches to $K = 1.75$, $\theta = 2.5$. The solid circles represent an average over 90 trajectories and the line is a best fit as indicated by (3.2) and below.

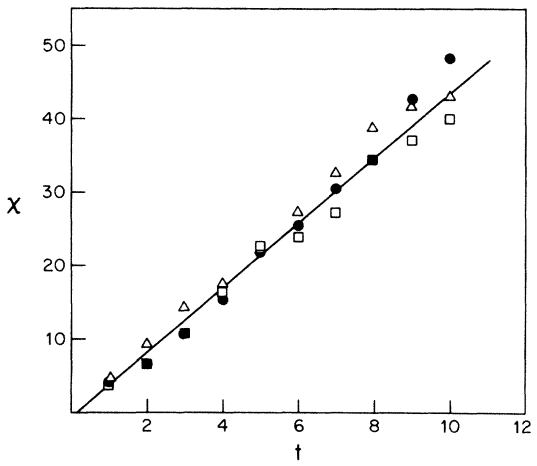

FIG. 5. Results for $\chi(t)$ at intermediate and long times for three kinds of initial conditions. (i) $\{\psi_i\} = 0$ (solid circles), (ii) random Ising (squares), and (iii) random uniform (triangles) (see text, Sec. II for details). All quenches are to $K = 1.75$, $\theta = 2.5$ and each set of points is a 30-run average. The straight line is the best overall linear fit. One sees that the initial conditions do not affect the intermediate- and long-time regions.

one can, for quenches into the ordering region, define a characteristic domain size $L(t)$ using

$$\chi(t) = L^d(t) = L^2(t) \tag{3.3}$$

in two dimensions. As stated in conjunction with (3.2) and Fig. 4, we find that for times $t \gg t_0$, where t_0 is always very small, $\chi(t) \propto (t - t_0)$. We therefore have that $L(t) \propto t^{1/2}$ at long times, in agreement with the LCA

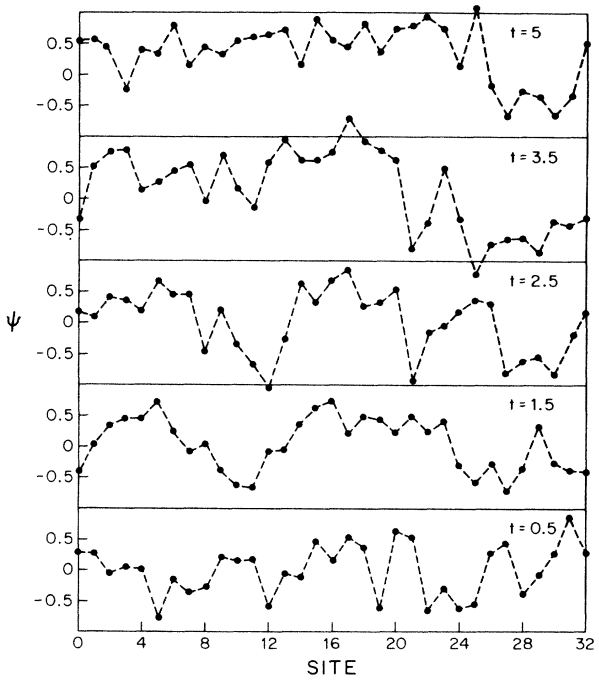

FIG. 6. Evolution of a typical row of $\psi_i(t)$ on the square lattice, for a quench to $K = 1.75$, $\theta = 2.5$. One can see that this particular row largely becomes part of a domain in which $\psi_i(t)$ is positive.

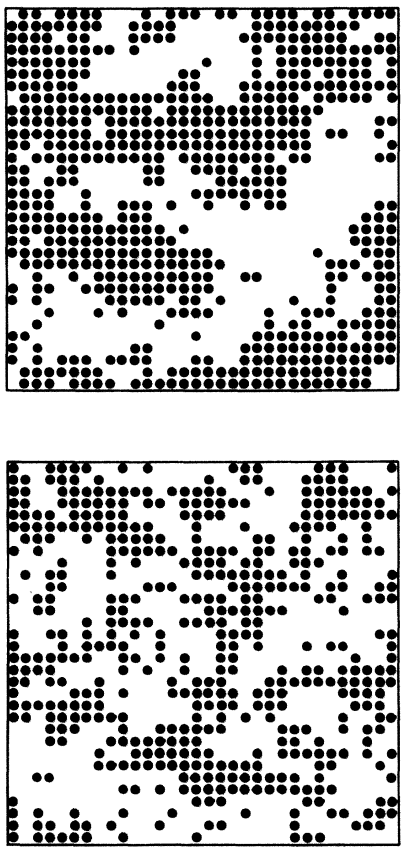

FIG. 7. Another picture of the same run as in Fig. 6 at times $t=0.5$ (lower panel) and $t=5$ (upper panel). The dots represent sites where $\psi_i > 0$. The row plotted in Fig. 6 is the twelfth from the top.

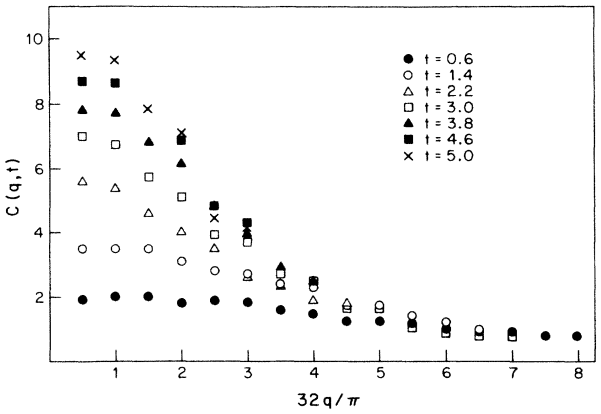

FIG. 8. Evolution of the central peak: the circularly averaged $C(q,t)$ at several times as indicated. The results represent an average over 60 trajectories for quenches to $K=0.8$, $\theta=12$.

law.[11] Although we have chosen the K,θ pairs (1.75, 2.5) and (0.8, 12) for particularly detailed analysis (as is obvious from the figures), we have verified the $\chi \propto t$ law for values of (θ,K) over the entire ordered portion of the phase diagram and obtained the same long-time behavior for $L(t)$.

We can gain more-detailed quantitative information by studying $C(r_i-r_j,t)$ and $C(q,t)$. We plot the angular averaged $C(q,t)$ in Fig. 8 for $K=0.8$, $\theta=12$ and 60 runs, and a sequence of increasing times. One clearly sees the development of a central peak with a shrinking width. In Fig. 9 we have $K=1.75$ (a much lower temperature than in Fig. 8), $\theta=2.5$, and 30 runs. In this case the development of a central peak is even sharper. A second determination of the characteristic domain size can be made if one recognizes that the shrinking width of $C(q,t)$, q_w, as obtained from careful extrapolation of data such as that shown in Figs. 8 and 9, is inversely proportional to the domain size. In this case, we fit $q_w(t)$ to the form $q_w(t)=a'(t-t_0)^{-b}$, and taking t_0 from the fit to the corresponding χ data (i.e., the height of the peak) we determine the best exponent b. Exponents obtained in this way vary from 0.46 to 0.56 in satisfactory agreement with the LCA law. We have, as an alternative, attempted to pin down $q_w(t)$ by numerically calculating the first moment of $C(q,t)$. The results depend on cutoff chosen unfortunately, because the "tail" of $C(q,t)$ is noisy, but the exponents obtained are very near 0.5 if one uses no cutoff, that is, sums over the whole Brillouin zone when calculating the moment.

As one can anticipate from the growth laws for $q_w(t)$ and $X(t)$ given above, our results for $C(q,t)$ can be written in the scaling form:

$$C(q,t)=\chi(t)F(q/q_w(t)) \; . \tag{3.4}$$

The scaling function $F(x)$ for the circularly averaged $C(q,t)$ is, within statistical error, indistinguishable from that found in Ref. 1 for the Ising model (solid line in Fig.

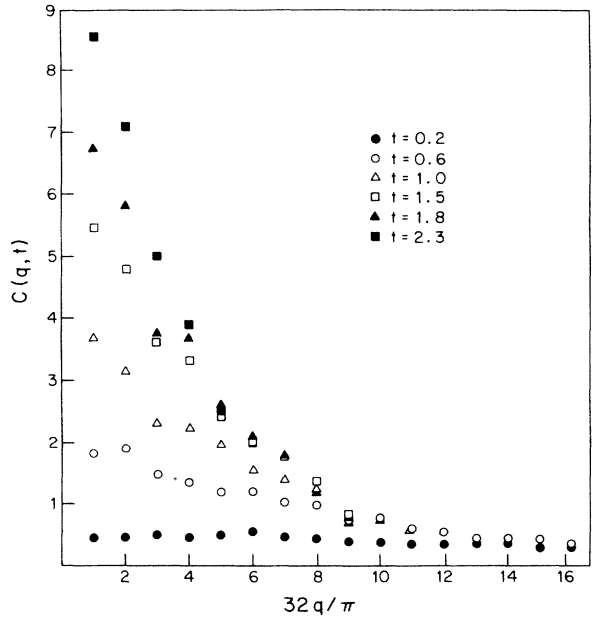

FIG. 9. Same as Fig. 8, but with $K=1.75$, $\theta=2.5$, and 30 runs.

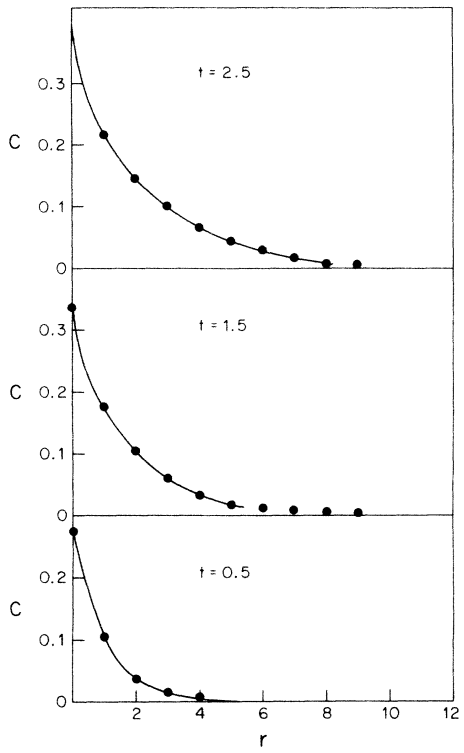

FIG. 10. The correlation function $C(r)$ along the x axis for a quench to $K=1.75$, $\theta=2.5$, at the times indicated. The lines are only a guide to the eye. The solid circles are 30 run averages.

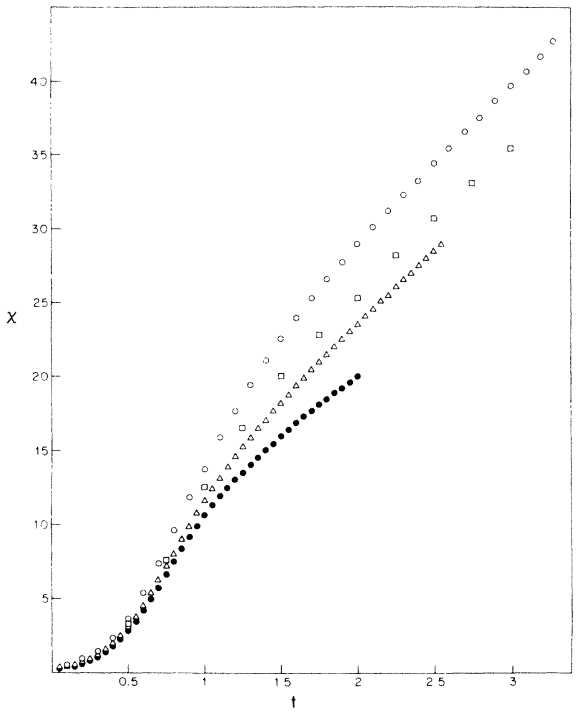

FIG. 11. $\chi(t)$ for quenches to zero temperature $J=1.75$, $\theta=2.5$ (see text). Each set of points represents 30 trajectories with random [type (iii), see text] initial conditions. Note how the long-time behavior appears to be extremely sensitive to initial conditions, in the absence of noise.

5 of Ref. 1), and it differs slightly but appreciably from the prediction of Ref. 13 (see dashed line in the same figure) in the range $1.5<x<4$.

The spatial dependence of correlation functions along the x axis and for three times is shown in Fig. 10 for $K=1.75$ and $\theta=2.5$. One clearly sees that larger regions are correlated as time proceeds.

Another matter of particular interest is the zero-temperature limit. In the Ising case the behavior of the system in that limit determines, by renormalization-group arguments,[18] the growth law. It is therefore important to check what happens in the present case.

With the parametrization used here, the zero-temperature limit would correspond to taking $K=\infty$ and the noise strength Γ finite. This is numerically impractical. Therefore, we take the physically more transparent route of writing explicitly $K=J/T$, $\Gamma=\Gamma' t'$, and taking $T\to 0$ while keeping J and Γ' finite. Our basic equations (2.5) and (2.6) remain the same except for replacing ΓK by $\Gamma' J$ in the deterministic terms and Γ by $\Gamma' T$ in the noise terms. At $T=0$ only the deterministic part of the equation remains. As is usually the case with nonlinear equations, the solutions are extremely sensitive to the initial conditions. Initial condition (i) leads to $\{\psi_i(t)\}\equiv 0$ which is unphysical and also unstable. We believe that the physics is best represented by averaging over many trajectories with type-(iii) initial conditions. The results of doing this [for $J=1.75$, $\theta=2.5$ and the time in units of $(\Gamma')^{-1}$] are shown in Fig. 11, for four 30-run sets of results for $\chi(t)$. We see that for the same number of trajectories, the deterministic trajectories fluctuate much more than those obtained in the presence of noise, where 30 runs are usually enough to obtain fairly satisfactory convergence. Further, the region of linear growth is very short. The early-time region is expanded and χ starts bending towards saturation earlier than at higher tempertures.

To further investigate this limit we consider next (Fig. 12) very low but nonzero temperatures. The curves in Fig. 12 correspond to the same conditions as Fig. 1 but with $T=0.1$ (i.e., $K=17.5$) and $T=0.5$ ($K=3.50$). Note that in the Ising case these would correspond to values of the usual low-temperature variable $y=e^{-4K}$ of 10^{-31} and 10^{-6}, respectively, which are very small indeed. However, in the continuum case the appropriate low-temperature variable is $1/K$, the second value behaves quite normally and even the first shows clear linear growth at intermediate times, even though there is a "shoulder" near $t=1$. It seems that when the noise is weak it takes longer for its influence to be felt.

For $T_F\neq 0$ the system is rather insensitive to initial conditions, that is, memory of the initial conditions is destroyed by the noise within a very short time. For $T_F=0$ the initial conditions are the disordering agent. Our conclusion is that the initial conditions seem to be much less efficient than noise in randomizing the system. This may mean that one would need to average at zero temperature over a number of runs much larger than at finite temperature. This would be reminiscent of the SFKI case, where

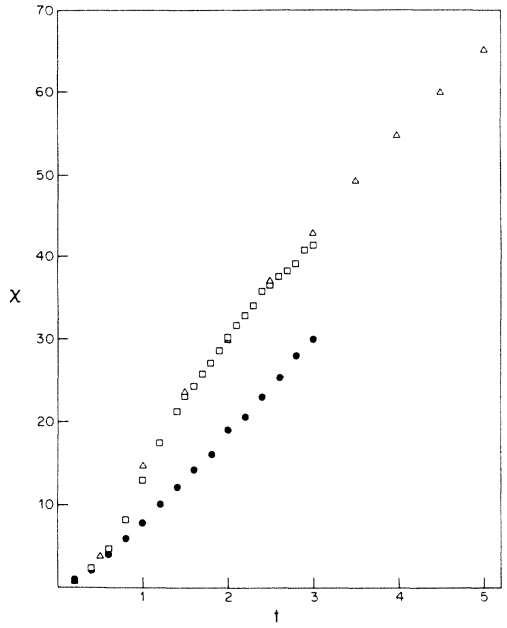

FIG. 12. $\chi(t)$ for quenches to low but finite temperature. The quantities K and θ are as in Fig. 11, but the temperature is now $T=J/K=0.1$ (squares and triangles) and $T=0.5$ (solid circles). Each set of points represents 30 runs. Note that there is now no problem with convergence, even at the lowest temperature.

$\chi(t)$ is very unstable. Alternatively, it is also possible that one must consider the limit $T\rightarrow 0$, i.e., when a small but finite amount of noise is present, as distinct from the purely deterministic case. Clearly this matter will need further study.

Finally, we turn to the question of comparing this method with MC techniques. Since the Ising limit ($\theta\rightarrow\infty$) for the Langevin equation is nonergodic, we cannot compare with simulations in the Ising case. However, one can perform the simulations directly with the free energy (2.1) by choosing a site i at random, attempting to change ψ_i by an amount $\delta\psi_i$ randomly distributed between $-\delta\psi_0$ and $\delta\psi_0$, and accepting the change with probability proportional to $e^{-\delta F}$. The comparison between this MC procedure and direct solution of the Langevin equation has been discussed in Ref. 17. They study a different model, but their conclusions should apply to our case, at least semiquantitatively, which is all we need for our purposes. It turns out that the two methods will give equivalent results in the limit where $|\delta\psi_0|\rightarrow 0$, provided that Γ is not too small. Within our units and conventions, the correspondence between MC time $t_{\rm MC}$ in step per site and Langevin equation time t is given approximately by

$$t_{\rm MC}\simeq\frac{12t}{|\delta\psi_0|^2}\ . \tag{3.5}$$

If one takes $|\delta\psi_0|=0.5$, which seems to be the largest reasonable size for the model of Ref. 17, one gets that one of our units of time is about 5000 steps per site, and following the system to time $t=10$ would be about 50 000 MC steps. We emphasize that these are only order-of-magnitude estimates.

Assuming δt as small as 0.005 (and we usually do not need such a small step) we have 200 integration steps in our time unit. Therefore our procedure will be more efficient than the MC algorithm unless the algebra involved in each integration step is 25—50 times slower than the corresponding algebra in one MC step. This is certainly not the case, as one can see from a rough count of the number of floating point operations involved in each case. This assumes that the number of runs needed in each case is roughly the same.

An additional argument can be given in support of our contention that the direct method compares in effectiveness with MC. We have seen that for the quenches considered here correlations grow up to a distance of 32 units in a time $t\sim 5$. For the Ising model[18] the corresponding times are larger than 10^4 steps. Thus, the time range considered here is, in a sense, long when compared with MC times.

IV. CONCLUSIONS

We have shown that direct numerical solution of Langevin equations can be quite useful in treating the growth kinetics of an order-disorder transition. One recovers the expected results, such as the Lifshitz-Cahn-Allen law. The amount of computing required appears to be at least competitive with that needed for the simulations, provided that proper attention is paid to the need for a fast generator of Gaussianly distributed random numbers.

It is obviously of interest to apply this procedure to other models. We are currently working on the case of spinodal decomposition, where, in the pure Ising case, our RG analysis leads to a logarithmic law[7] rather than to a power law. The potential of the method for use in other situations (such as discussed in the Introduction) is now quite clear.

ACKNOWLEDGMENTS

This work was supported in part by the Microelectronics and Information Sciences Center at the University of Minnesota and by NSF Grant No. DMR 8316616 at the University of Chicago. A grant of computer time from the Supercomputer Institute at the University of Minnesota is gratefully acknowledged.

[1]F. C. Zhang, O. T. Valls, and G. F. Mazenko, Phys. Rev. B **31**, 1579 (1985).

[2]P. A. Shani, G. S. Grest, M. P. Anderson, and D. J. Srolovitz, Phys. Rev. B **28**, 2705 (1983).

[3]G. S. Grest, D. J. Srolovitz, and M. P. Anderson, Phys. Rev. Lett. **52**, 1321 (1984).

[4]G. F. Mazenko and M. Zanetti, Phys. Rev. Lett. **53**, 2106 (1984).

[5]O. Mauritsen, Phys. Rev. Lett. **56**, 850 (1986).

[6]G. F. Mazenko, O. T. Valls, and F. C. Zhang, Phys. Rev. B **32**,

5807 (1985).
[7]G. F. Mazenko and O. T. Valls, Phys. Rev. B **33**, 1823 (1986).
[8]R. Petschek and H. Metiu, J. Chem. Phys. **79**, 3443 (1983).
[9]P. Hohenberg and B. Halperin, Rev. Mod. Phys. **49**, 435 (1977).
[10]J. Langer, Ann. Phys. (N.Y.) **41**, 108 (1967).
[11]J. W. Cahn and S. M. Allen, J. Phys. (Paris) Colloq. **C7**, 54 (1977); S. M. Allen and J. W. Cahn, Acta Metall. **27**, 1085 (1979).
[12]K. Kawasaki and J. Gunton, in *Progress in Liquid Physics* (Wiley, Chichester, 1976).
[13]T. Ohta, D. Jasnow, and K. Kawasaki, Phys. Rev. Lett. **49**, 1273 (1982).
[14]S. K. Ma, *Modern Theory of Critical Phenomena* (Benjamin, Reading, Mass., 1976).
[15]P. D. Beale, S. Sarker, and J. A. Krumhansl, Phys. Rev. B **24**, 266 (1981).
[16]See formula 26.2.22 in *Handbook of Mathematical Functions*, edited by M. Abramowitz and I. Stegun (Dover, New York, 1972).
[17]D. Meakin, H. Metiu, R. G. Petschek, and D. J. Scalapino, J. Chem. Phys. **79**, 1948 (1983).
[18]G. F. Mazenko and O. T. Valls, Phys. Rev. B **30**, 6732 (1984).